Supporting information file

Design, Synthesis, Molecular Docking and Anticancer Activity of Benzothiazolecarbohydrazide-Sulfonate Conjugates: Insights into ROS-Induced DNA Damage and Tubulin Polymerization Inhibition

Chemistry

Melting points were recorded on a Stuart SMP30 melting point apparatus. IR spectra (KBr) were recorded on a JASCO 6100 spectrophotometer. NMR spectra were recorded on a JEOL AS 500 (^{1}H: 500 MHz, ^{13}C: 125 MHz) and spectrometer. Mass spectra were recorded on a Shimadzu GCMS-QP 1000 EX (EI, 70 eV) spectrometer, Elemental microanalyses were recorded on a Vario El Elementar analyzer. All spectral analyses were conducted at National Research Centre, Dokki, Cairo, Egypt.

Anti-Cancer Activity

Cell Lines

Human colorectal carcinoma (HCT-116 cell line), human breast carcinoma (MCF-7 cell line), human prostate cancer (PC3 cell line), and normal human cell line (BJ-1); A telomerase-immortalized normal foreskin fibroblast cell line was originally obtained from ATCC (American Type Culture Collection) and kindly gifted to us by the Karolinska Center, Department of Oncology and Pathology, Karolinska Institute and Hospital, Stockholm, Sweden.

Cell Viability Assay

This was done according to [1]. The cells were seeded at a concentration of 10 *10^3 cells per well in the case of MCF-7 and PC3, 20*10^3 cells/well in the case of the HCT-116 cell line and 35–45*10^3cells/well in the case of BJ-1 using 96-well plates at 37°C. After 48 h of incubation, the medium was aspirated and 40 μL MTT salt (2.5 mg/mL) was added and further incubated for 4 h. Then, 200 μL of 10% sodium dodecyl sulfate (SDS) was added. The absorbance was measured at 595 nm. 5-fluorouracil was used as a positive control. A negative control, composed of DMSO, was also used.

Determination of IC_{50} Values

IC_{50} values were calculated, using a probit analysis, and by utilizing the SPSS computer program (SPSS for Windows, statistical analysis software package/version 9/1989 SPSS Inc., Chicago, IL, USA).

Human Reactive Oxygen Species (ROS) estimation

The micro ELISA plate in this kit is pre-coated with the desired specific antibody to be detected. Amsbio kit was used with Catalogue Number: AMS.E01R0021.

Enzyme-linked Immunosorbent Assay Kit for Tubulin Beta (TUBb).

The MCF-7 cells were inoculated with 6i compound for 24 hours, followed by the addition of Avidin conjugated to Horseradish Peroxidase (HRP) to each microplate well and incubated. After the addition of the TMB substrate solution, the wells containing TUBb, enzyme-conjugated Avidin and biotin-conjugated antibody revealed a color change. The addition of sulphuric acid solution terminated the enzymatic reaction. The color change was measured spectrophotometrically at a wavelength of 450 nm ± 10 nm [2].

2.1. Estimation of DNA Fragmentation through DPA assay

Assessment of DNA fragmentation of the cells was done, as described by the reported method [3]. Briefly, the cells were lysed for 15 min on ice with 0.5% (v/v) Triton X-100, 20 mM EDTA and 5 uM Tris (pH 8.0). Then, the cells were centrifuged to separate intact chromatin from DNA fragments for 20 min, at 27,000 Xg. Measurement of the amount of DNA was done using a diphenylamine reagent and the optical density was measured at 600 nm.

Cell cycle analysis and apoptosis detection

Cell cycle analysis and apoptosis detection were carried out by flow cytometry. MCF-7 cells were seeded at $1\text{-}5\times10^4$ and incubated at 37 °C, 5% CO_2 overnight, After treatment with the tested compound 11, for 24 h, cell pellets were collected and centrifuged (300×g, 5 min). For cell cycle analysis, cell pellets were fixed with 70% ethanol on ice for 15 min and collected again [4]. The collected pellets were incubated with propidium iodide (PI) staining solution at room temperature for 1 h. Apoptosis detection was performed by Annexin V-FITC apoptosis detection kit (BioVision, Inc, Milpitas, CA, USA) following the manufacturer's protocol. The samples were analyzed using a FACS Calibur flow cytometer (BD Biosciences, San Jose, CA).

Docking

The three-dimensional (3D) coordinates of α/β-tubulin heterodimer in complex with nocodazole (PDB code: 7Z2P) were downloaded from Protein Data Bank. The receptor preparation was performed by deletion of all chains other than chains A and B followed by the deletion of all water molecules, ions, and other small molecules. Polar hydrogens were added while non-polar hydrogens were merged to their heavy atoms, Kollman Charges were assigned and finally, the receptor was saved in PDBQT format for molecular docking. Compound **6i** was sketched using ChemBioDraw Ultra 14.0 software (CambridgeSoft corporation), then energy minimized by MMFF94x Force Field in gas and saved in PDBQT format. Grid box with the size of 20 X 20 X 20 Å and grid spacing of 0.375 Å was centered on co-crystalized ligand at X=16.7, Y=64.9 and Z=37.6. docking simulation was performed using Autodock 4.2 with default parameters. The docking poses were ranked according to their docking scores, and the best energy pose was selected. Discovery Studio Visualizer v21.1.0.20298. Discovery Studio Visualizer v21.1.0.20298 was used to analyze the results and to study the interactions between the investigated compounds and the target receptors [5].

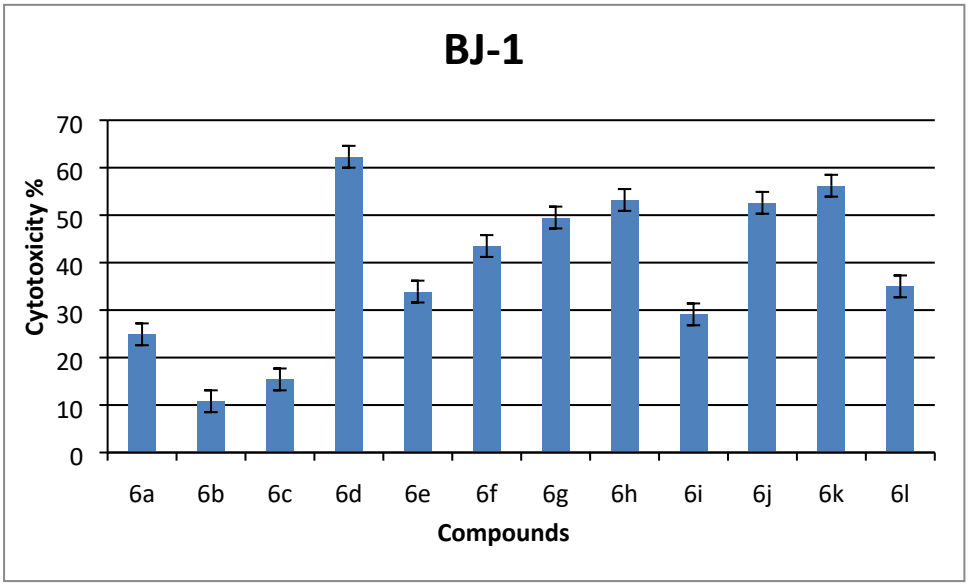

Figure S1: Cytotoxicity % of compounds on normal cells (BJ-1) at 100 µM, Values shown are mean ± S.D. (n = 3).

Table S1: Cytotoxicity % of the synthesized conjugates **6a-l** against three human tumor cell lines MCF-7, HCT-116 and PC3 at 100 μM. Data is an average of three readings ± Standard deviation

Compd. ID	Cytotoxicity %			
	MCF-7	**HCT-116**	**PC3**	**BJ-1**
6a	38.1±1.1	50±0.8	39.6±1.9	24.9
6b	16.6±0.6	44.6±2.4	29.4±1.1	10.8
6c	58.1±2.7	33.5±0.7	25.1±0.7	15.4
6d	62.5±3.1	66.7±2.6	66.5±2.2	62.3
6e	49.1±2.4	61.1±1.8	60.8±1.9	33.9
6f	32.3±0.9	62.8±1.9	44.5±2.2	43.5
6g	62.3±3.5	68.6±3.4	74.8±2.4	49.5
6h	40.5±2.2	55.2±0.9	63.4±1.9	53.2
6i	53.4±1.7	35.5±1.4	32±0.6	29.1
6j	46.6±1.8	68.5±3.7	62.3±1.8	52.6
6k	59.6±2.9	77.2±3.2	64.6±2.2	56.2
6l	26.3±1.9	42.7±2.4	33±1.3	35
5- FU	71.2±2.1	84.6±1.3	10.7±0.9	-

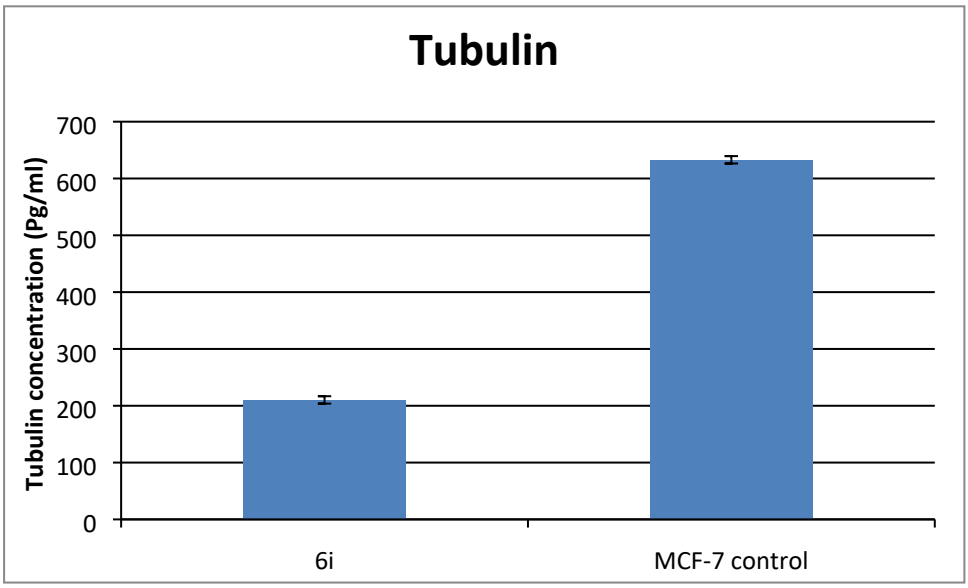

Fig. S2: Tubulin B estimation of treated MCF-7 with **6i**, compared to untreated cells.

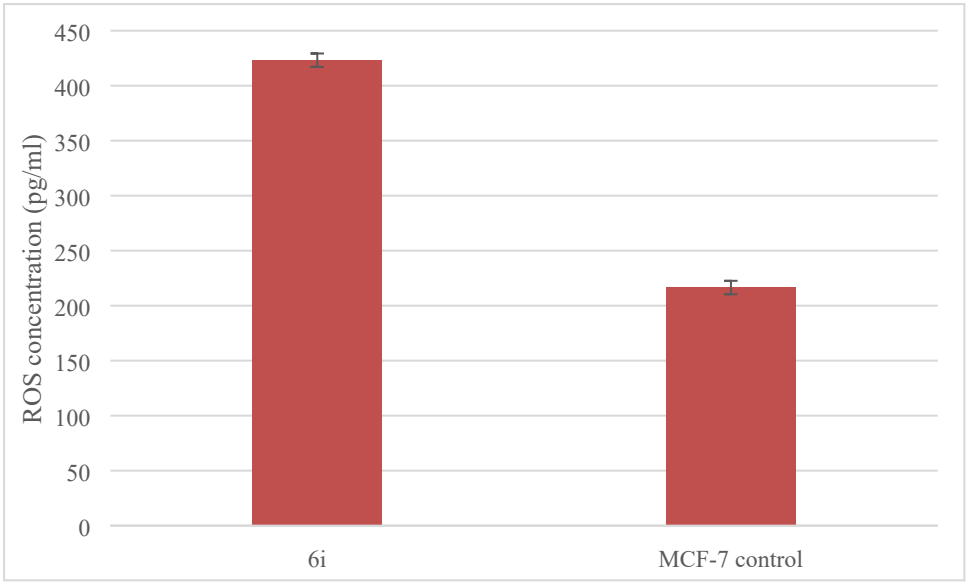

Fig. S3: ROS estimation of treated MCF-7 with **6i**, compared to untreated cells.

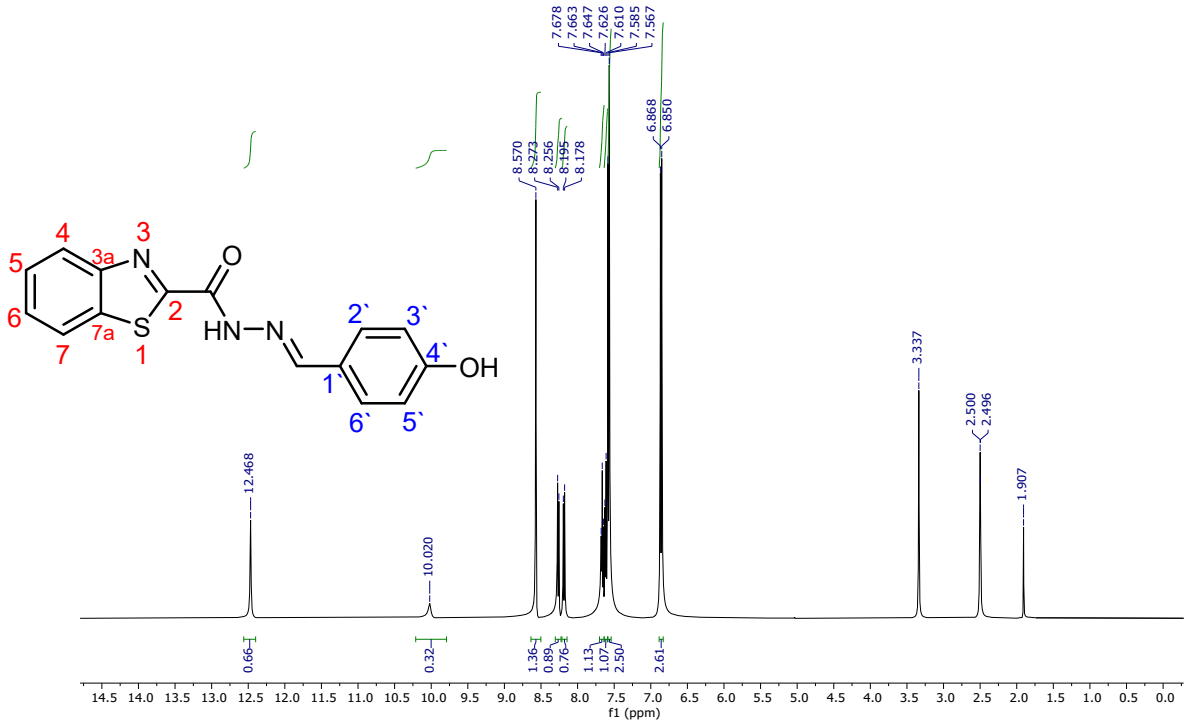

Fig. S4. ^{1}H NMR spectrum of compound **6a**.

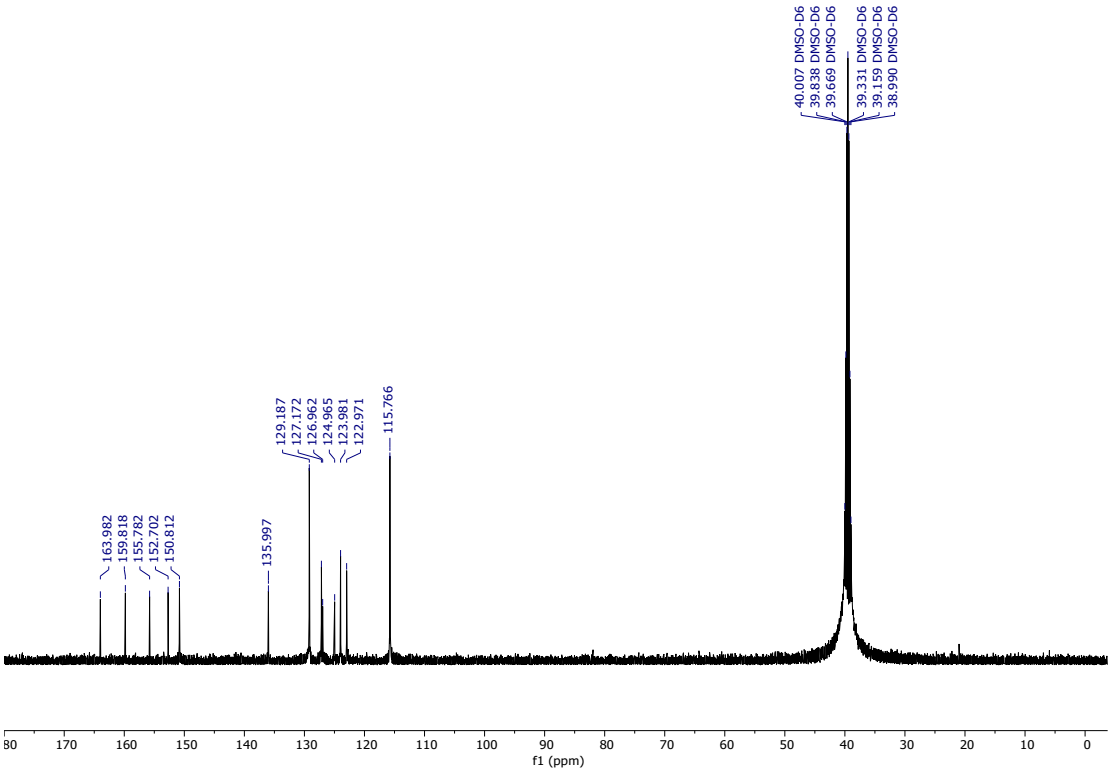

Fig. S5. ^{13}C NMR spectrum of compound **6a**.

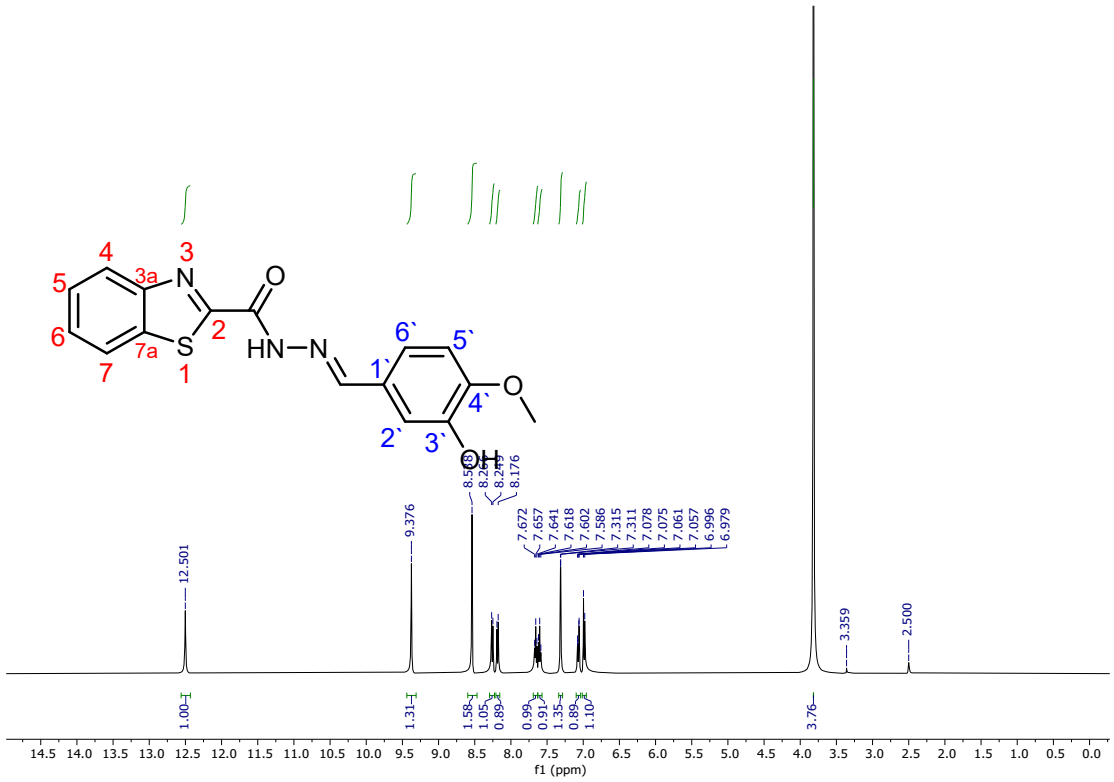

Fig. S6. ^{1}H NMR spectrum of compound **6b**.

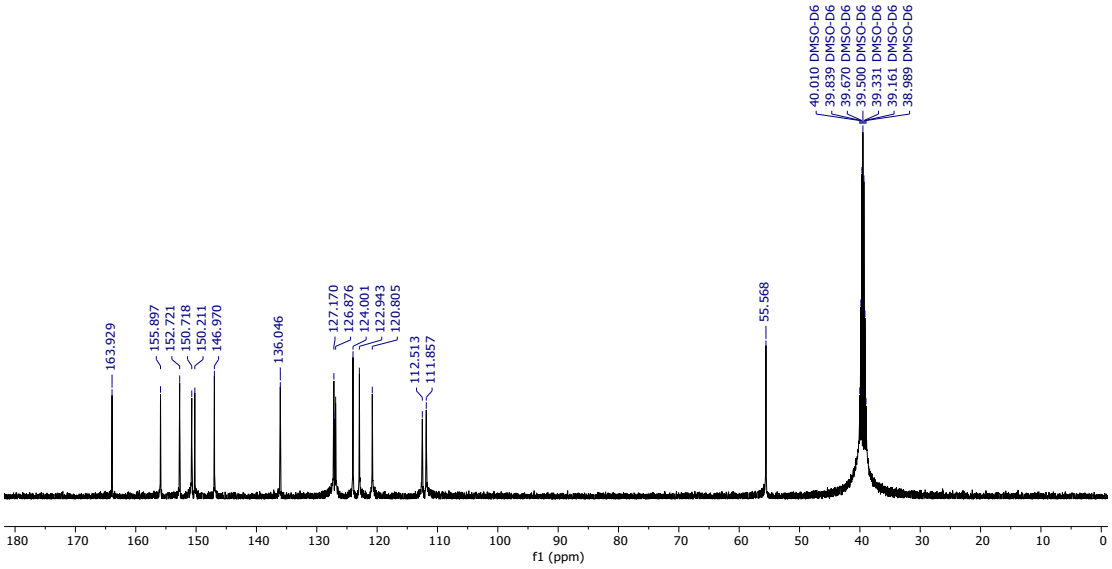

Fig. S7. ^{13}C NMR spectrum of compound **6b**.

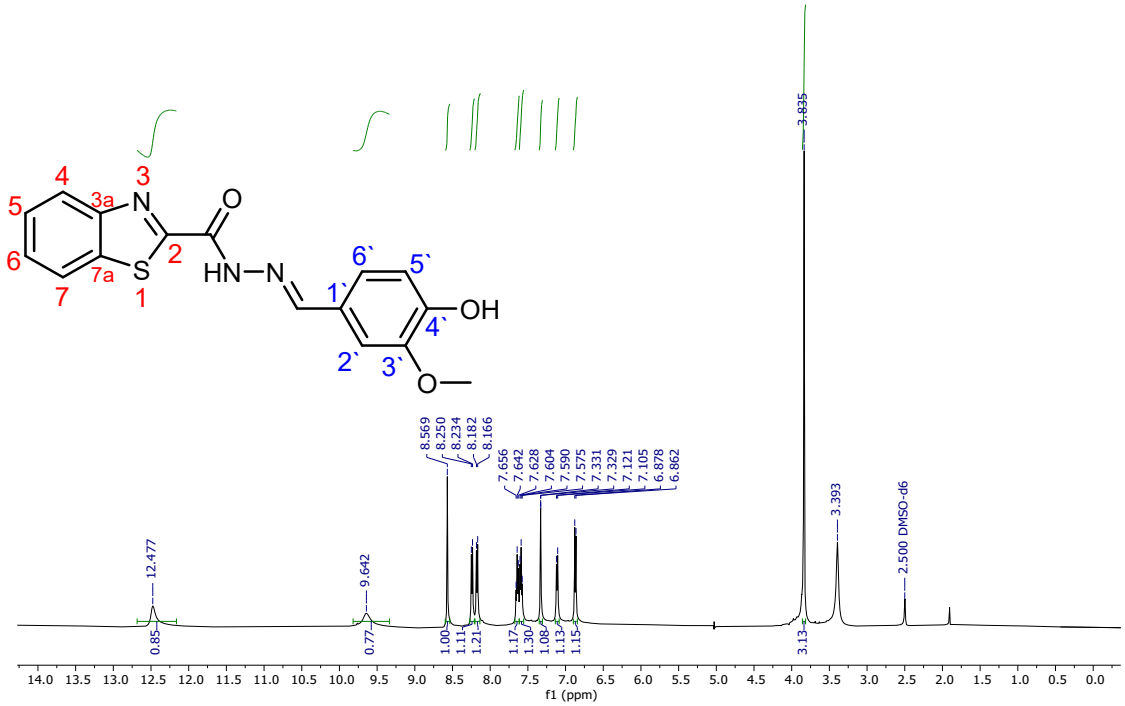

Fig. S8. ^{1}H NMR spectrum of compound **6c**.

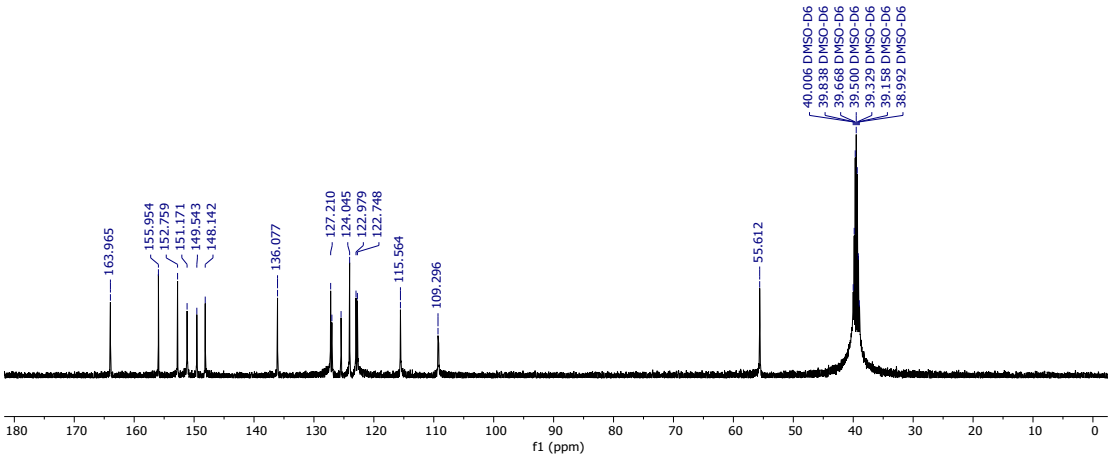

Fig. S9. ^{13}C NMR spectrum of compound **6c**.

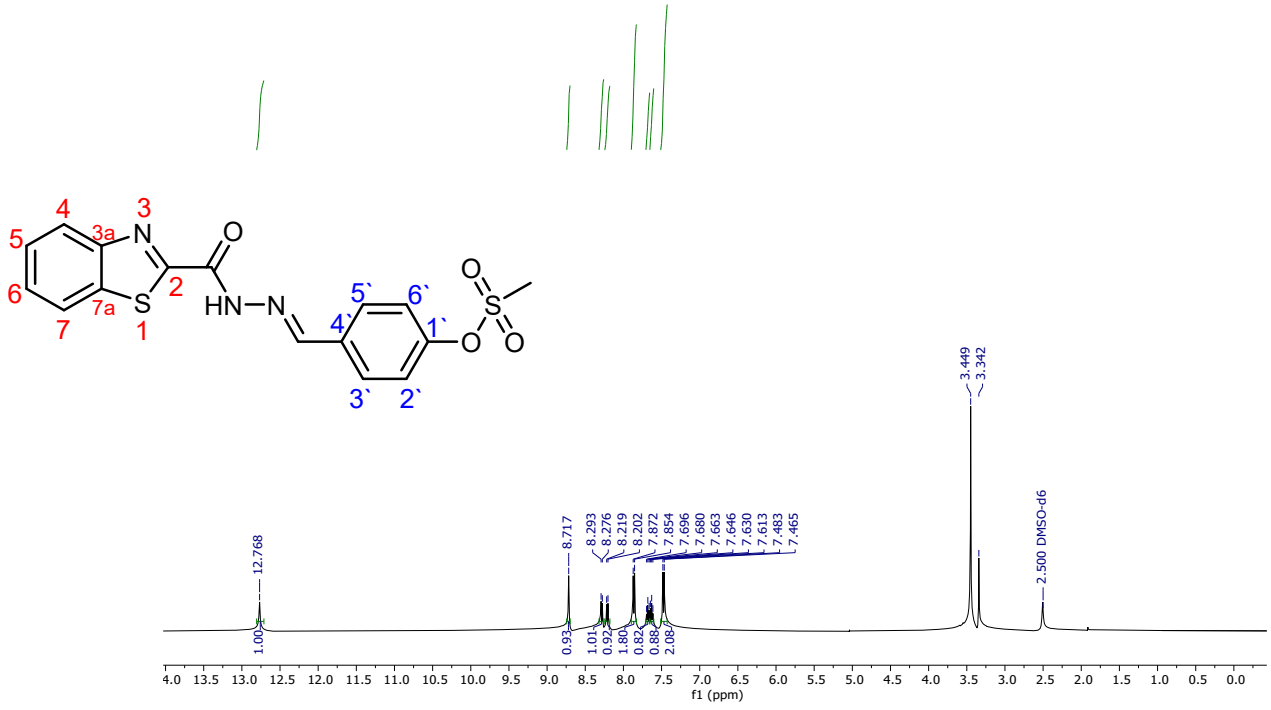

Fig. S10. ^{1}H NMR spectrum of compound **6d**.

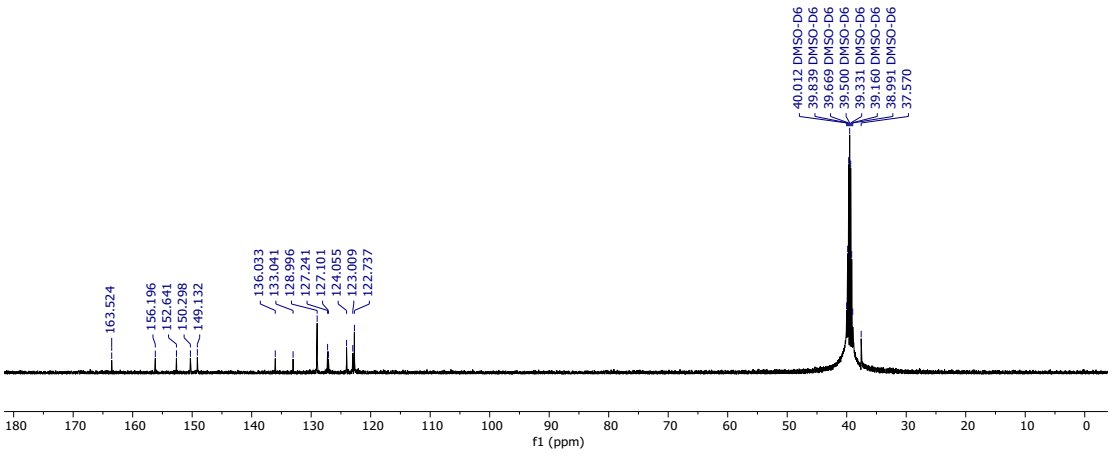

Fig. S11. ^{13}C NMR spectrum of compound **6d**.

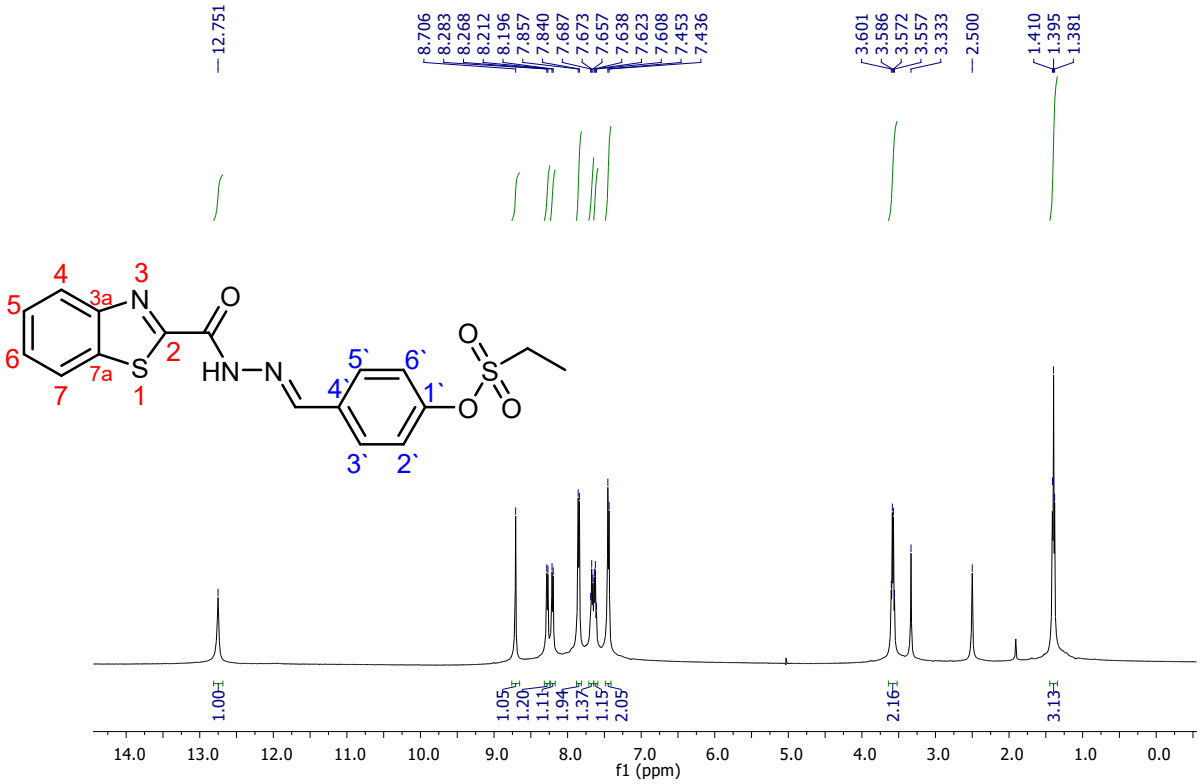

Fig. S12. ^{1}H NMR spectrum of compound **6e**.

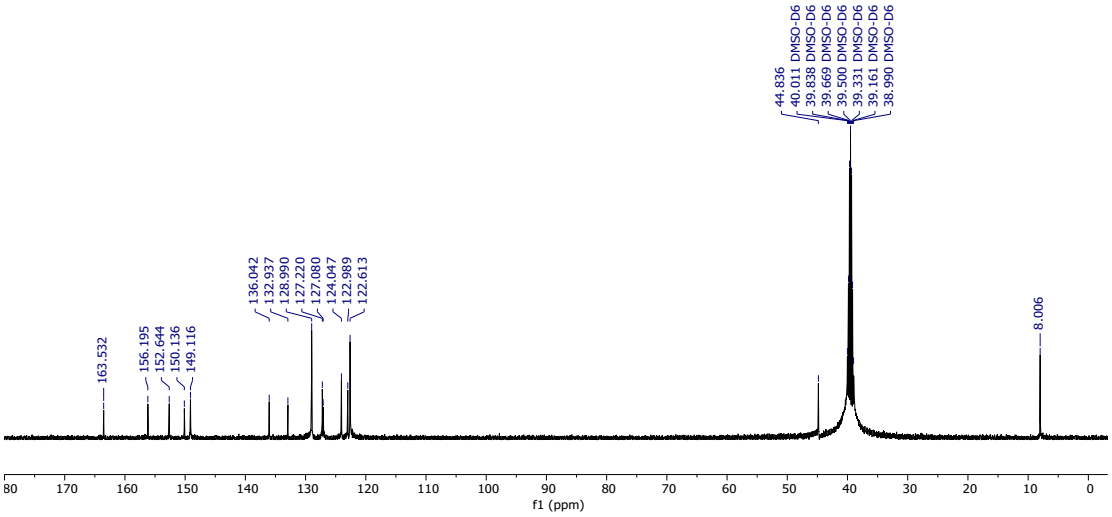

Fig. S13. ^{13}C NMR spectrum of compound **6e**.

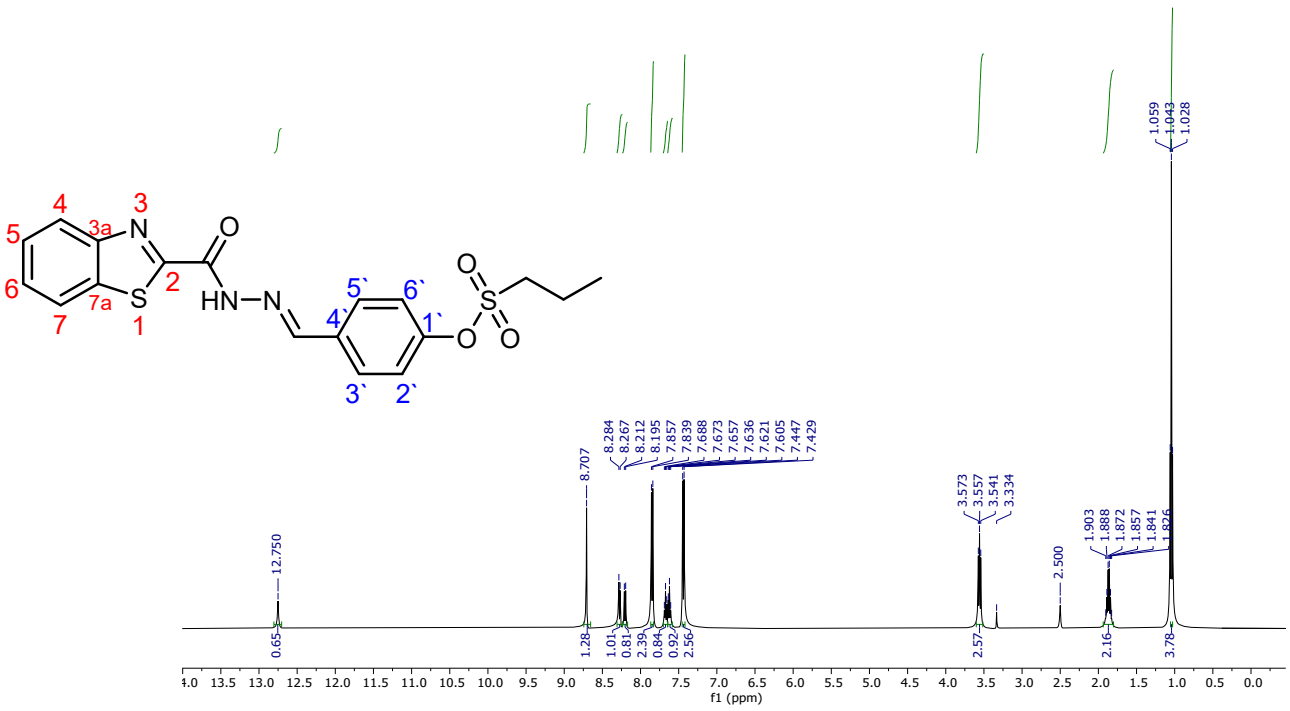

Fig. S14. ^{1}H NMR spectrum of compound **6f**.

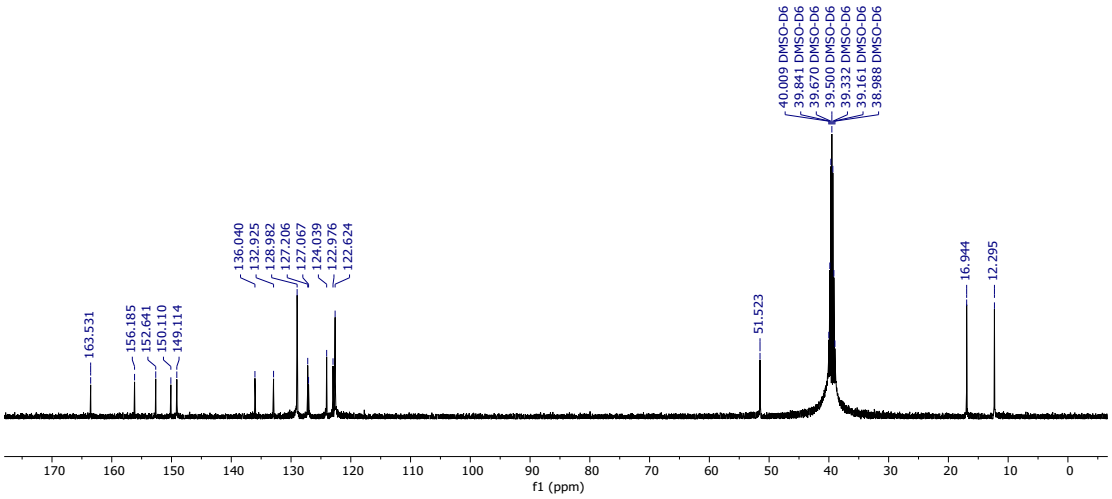

Fig. S15. ^{13}C NMR spectrum of compound **6f**.

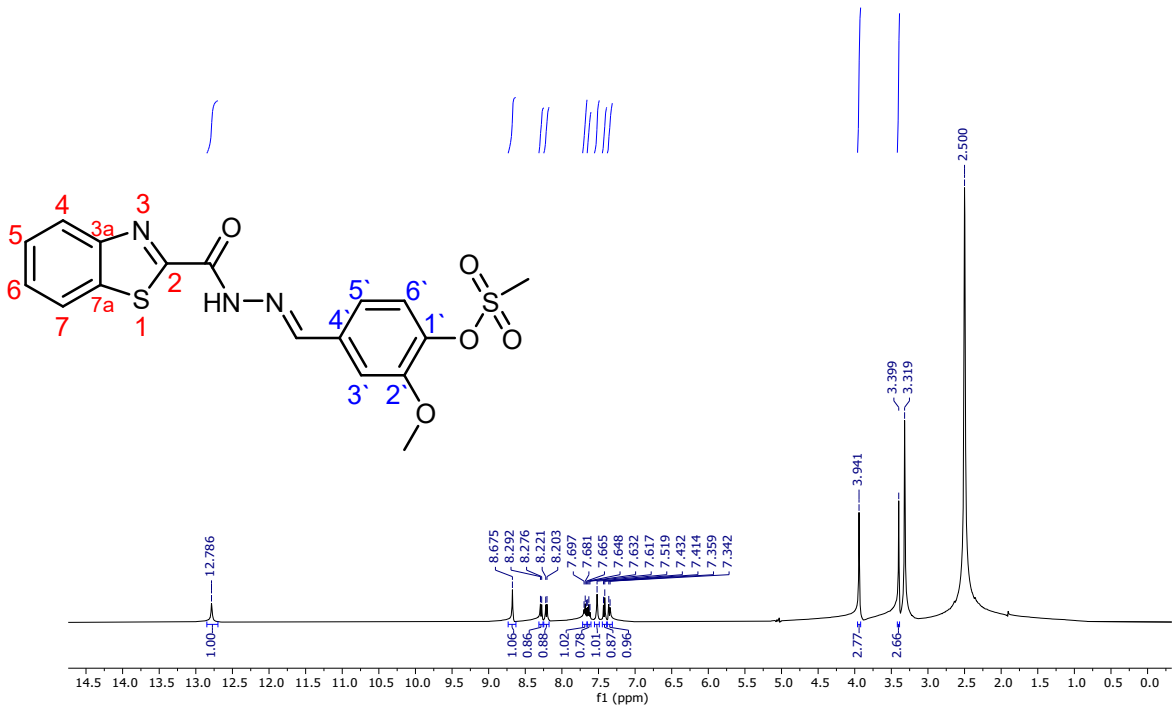

Fig. S16. ^{1}H NMR spectrum of compound **6g**.

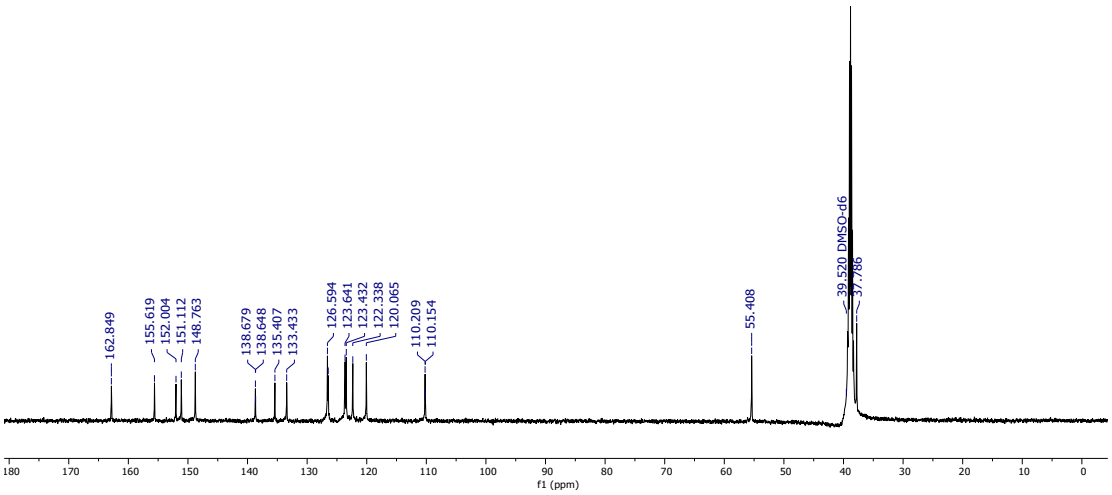

Fig. S17. ^{13}C NMR spectrum of compound **6g**.

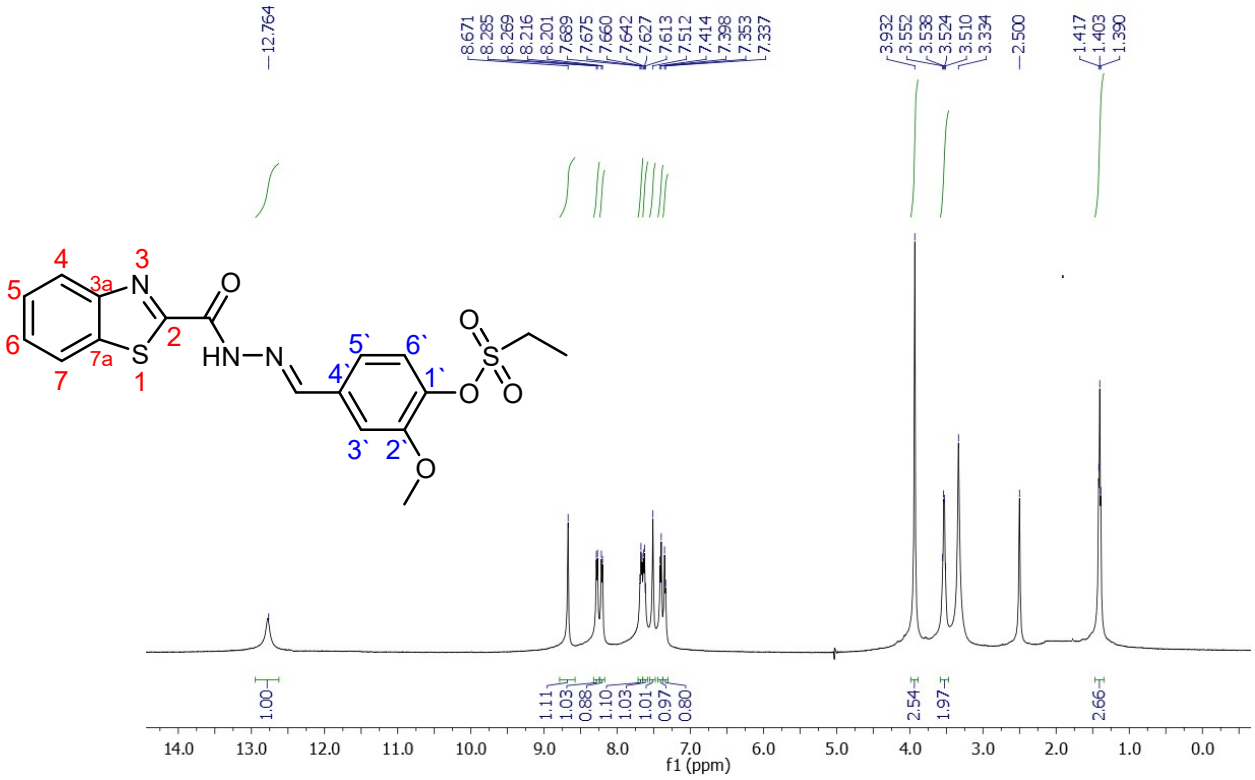

Fig. S18. ^{1}H NMR spectrum of compound **6h**.

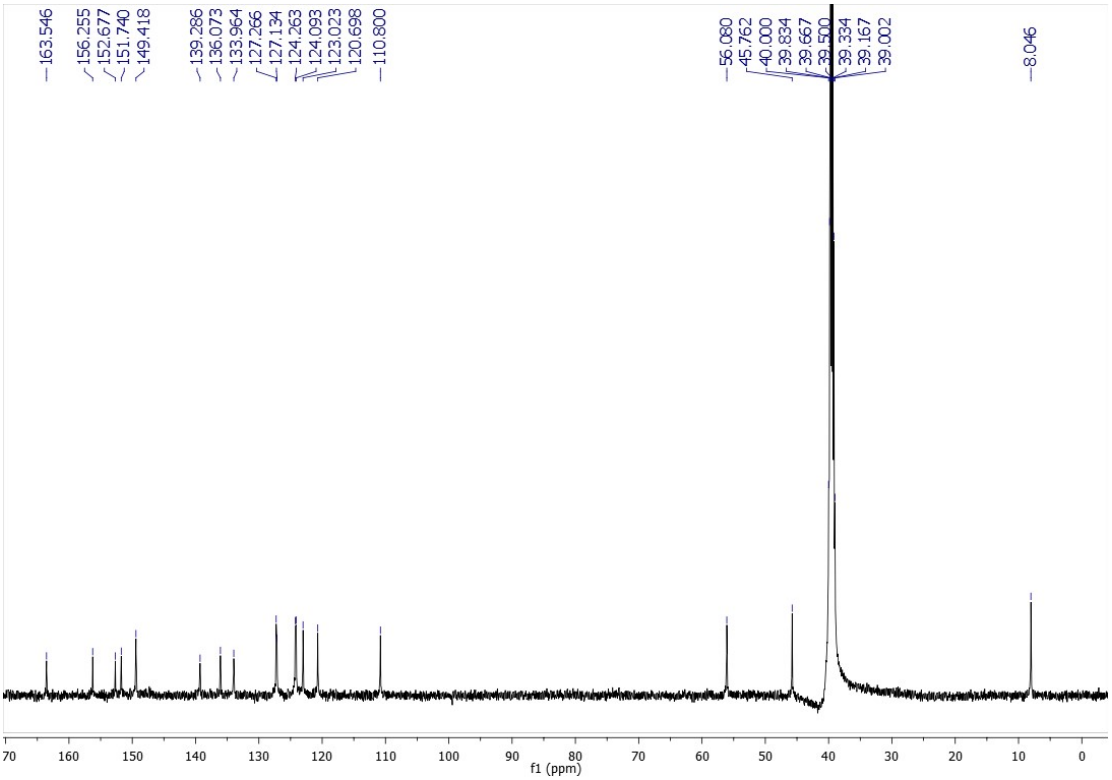

Fig. S19. ^{13}C NMR spectrum of compound **6h**.

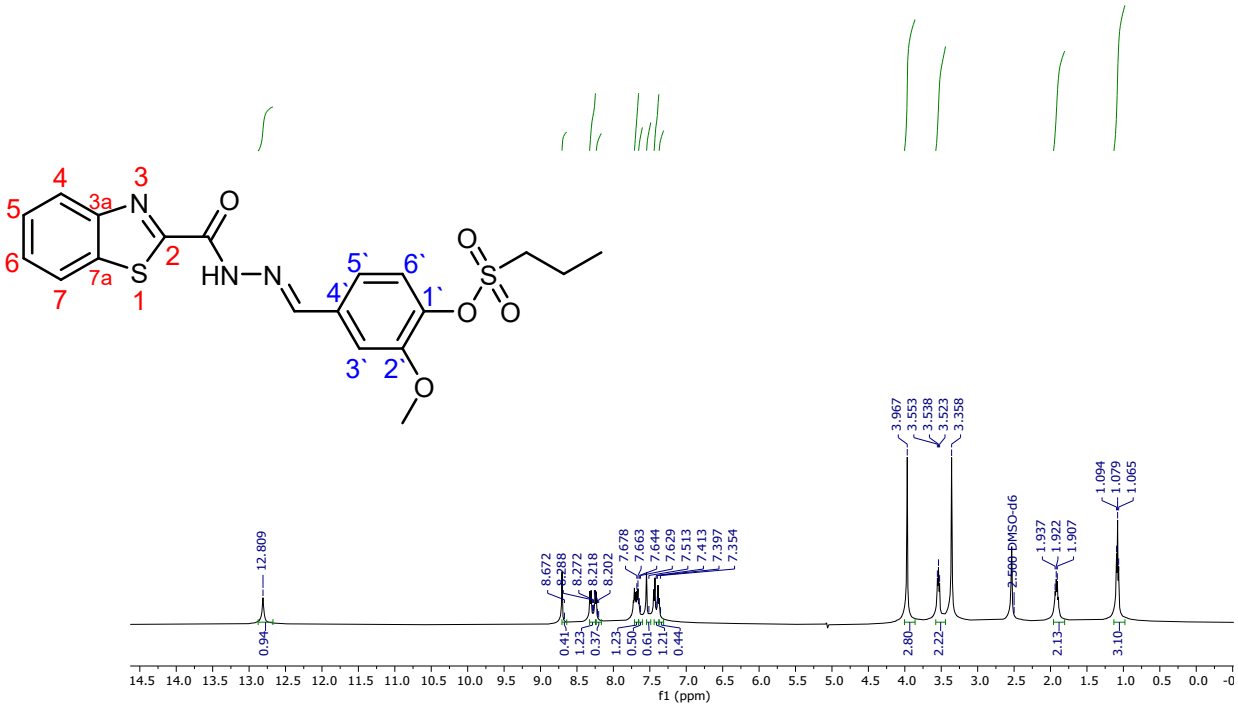

Fig. S20. ^{1}H NMR spectrum of compound **6i**.

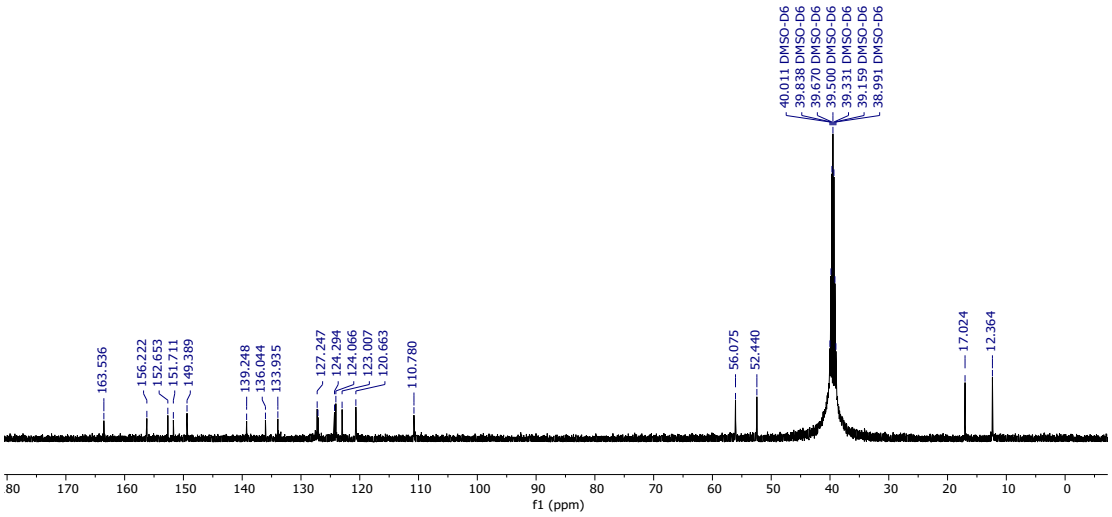

Fig. S21. ^{13}C NMR spectrum of compound **6i**.

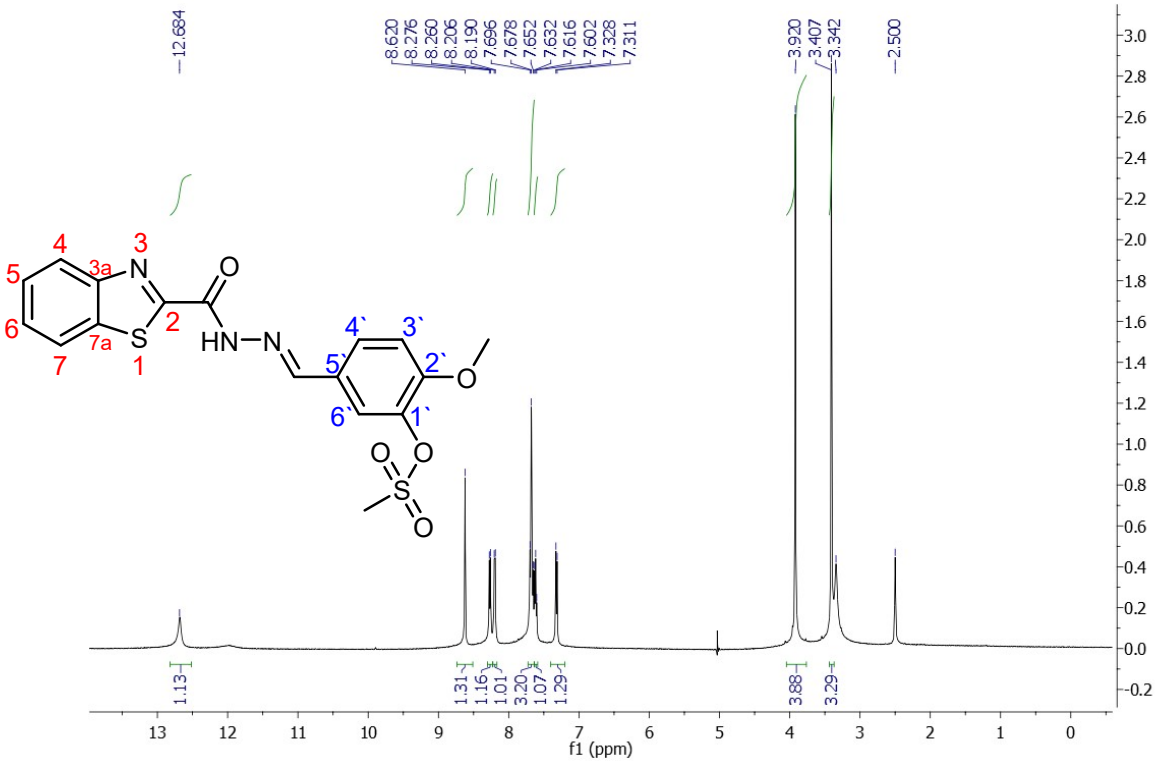

Fig. S22. ^{1}H NMR spectrum of compound **6j**.

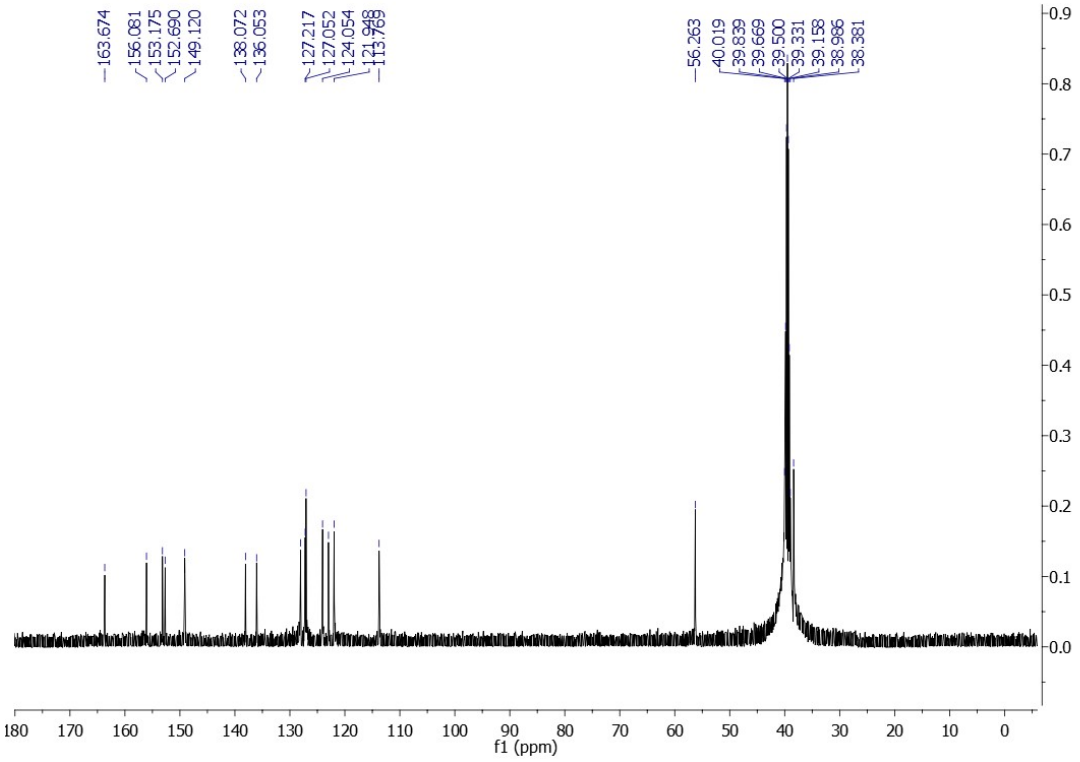

Fig. S23. ^{13}C NMR spectrum of compound **6j**.

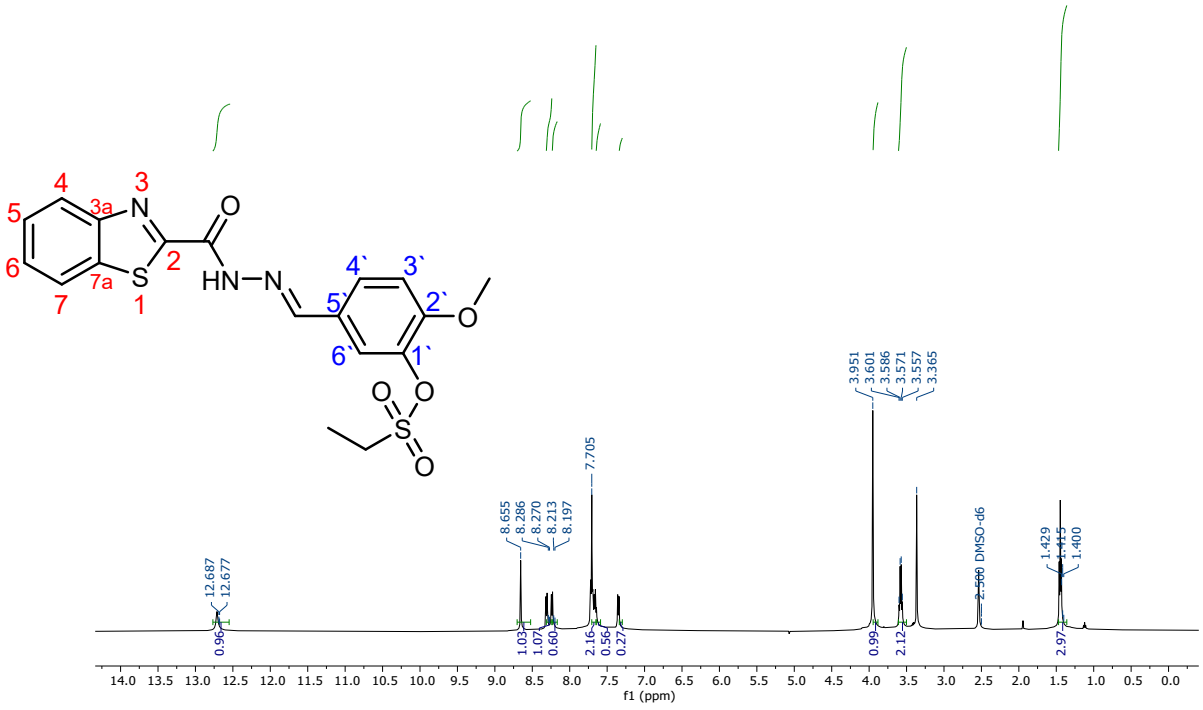

Fig. S24. ^{1}H NMR spectrum of compound **6k**.

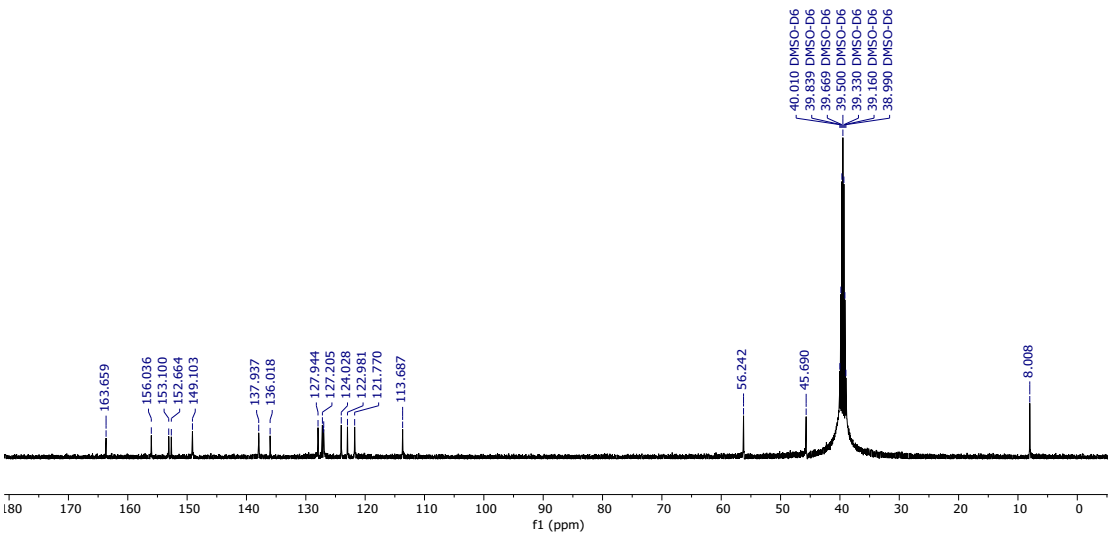

Fig. S25. ^{13}C NMR spectrum of compound **6j**.

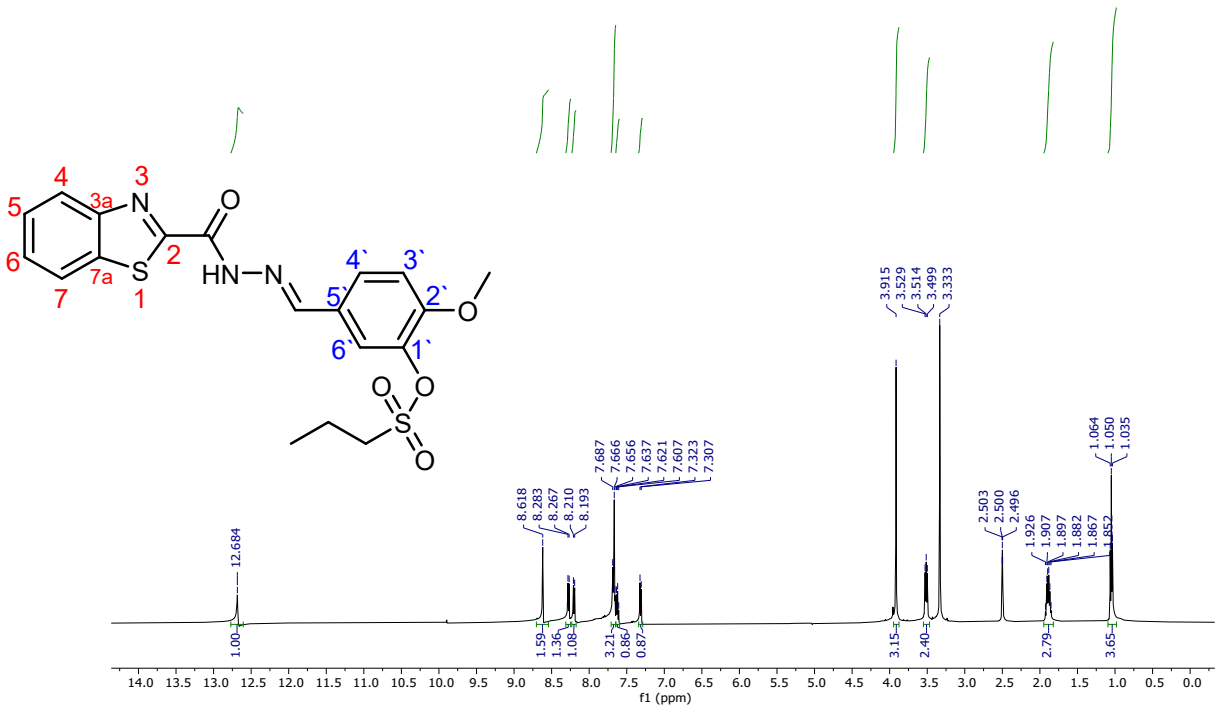

Fig. S26. ^{1}H NMR spectrum of compound **6l**.

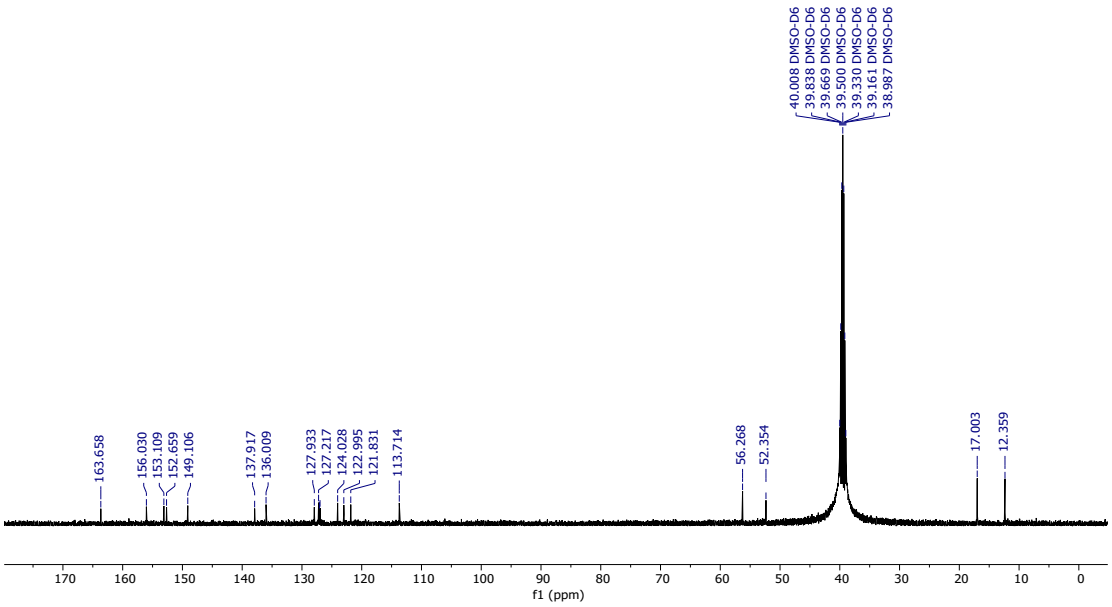

Fig. S27. ^{13}C NMR spectrum of compound **6l**.

References

1. Kassem AF, Omar MA, Temirak A, El-Shiekh RA, Srour AM. Barbiturate–sulfonate hybrids as potent cholinesterase inhibitors: design, synthesis and molecular modeling studies Future Med Chem. 2024;16(16):1615-1631. https://doi.org/10.1080/17568919.2024.2366158.
2. Khwaja S, Kumar K, Das R, Negi AS. Microtubule associated proteins as targets for anticancer drug development. Bioorg Chem. 2021;116:105320-36. doi: 10.1016/j.bioorg.2021.105320.
3. Nakamura H, Takada K. Reactive oxygen species in cancer: Current findings and future directions. Cancer Sci. 2021;112(10):3945-52. doi: 10.1111/cas.15068.
4. Kim SJ, Kim HS, Seo YR. Understanding of ROS-Inducing Strategy in Anticancer Therapy. Oxid Med Cell Longev. 2019;2019:5381692-12. doi: 10.1155/2019/5381692.
5. Zaidieh T, Smith JR, Ball KE, An Q. ROS as a novel indicator to predict anticancer drug efficacy. BMC Cancer. 2019;19(1):1224-1338. doi: 10.1186/s12885-019-6438-y.